Resolving Near-Seabed Velocity Anomalies: Deep Water Offshore South East India

Juergen Fruehn[1], Ian F. Jones[1], Victoria Valler[1], Pranaya Sangvai[2], Ajoy Biswal[2], and Mohit Mathur[2]

‘Geophysics’ special issue on
"Velocity Estimation for Depth Imaging"
(editor Bill Harlan)

Volume 73, NO.5, VE235-VE241

Corresponding author
Ian.Jones@iongeo.com

1 ION GX Technology, Egham, UK.

2 Reliance Industries Ltd., Mumbai, India.

ABSTRACT

Imaging in deep water environments poses a specific set of challenges, both in the data pre-conditioning and the velocity model building. These challenges include scattered complex 3D multiples, aliased noise, and low velocity shallow anomalies associated with channel fills and gas hydrates. In this paper, we describe an approach to tackling such problems for data from deep water off the north east coast of India, concentrating our attention on iterative velocity model building, more specifically the resolution of near surface and other velocity anomalies. In the region under investigation, the velocity field is complicated by narrow buried canyons (500 m wide) filled with low velocity sediments which give rise to severe pull-down effects; possible free gas accumulation below an extensive gas hydrate cap, producing dimming of the image below (perhaps as a result of absorption); and thin channel bodies with low-velocity fill. Hybrid gridded tomography using a conjugate gradient solver (with 20 m vertical cell size) is used to resolve small scale velocity anomalies (with thicknesses of about 50m). Manual picking of narrow channel features is used to define bodies too small for the tomography to resolve. Pre-stack depth migration using a velocity model built using a combination of these techniques was able to resolve pull-down and other image distortion effects in the final image. The resulting velocity field shows high resolution detail useful in identifying anomalous geobodies of potential exploration interest.

INTRODUCTION

Off the east coast of India, the transition from the shallower coastal waters to the deep shelf often encounters significant topographical variation in the sea bed, which gives rise to numerous effects which must be dealt with by the processing geophysicist. In addition to deep channels and steep slopes, we also encounter buried channels with low velocity fills and gas hydrates. Diffracted and “out-of-plane” multiples are the norm in these environments (Stewart, 2004), and must be dealt with in order to subsequently derive a reliable velocity model so as to deliver an acceptable structural image (Stewart et al, 2007). With the advent of 3D surface related multiple elimination (SRME), a theoretically robust approach to complex multiple attenuation has become available, and application of 3D SRME to these data proved to be very effective (Sangvai, et al, 2008; Smith et al, 2008). The SRME technique was pioneered by the Delft university consortium (Verschuur, et al, 1992), and involves generating a model of the multiples from the input data without prior knowledge of the velocity structure of the subsurface. Consequently, it is an ideal approach to accompany complex imaging problems, where an a-priori knowledge of the velocities can not be assumed.

In the data considered here, the water depths range from a few hundred metres to over 1 km, and for the most part are deeper than 1.5 km, with deeply incised sea-bed channels running down the continental slope. The region under consideration is roughly 42 km by 54 km (some 2200 sq.km) covering a large exploration area of unknown hydrocarbon potential. Figure 1 shows a survey outline, indicating the locations of various inlines and crosslines discussed in this paper. Also seen in the lower left of the figure is a canyon fill geobody described later. The data were collected in 2004, and imaged after 2D demultiple using 3D pre-stack time migration (preSTM). This time domain imaging produced very good results overall, but for certain specific parts of the region was considered sub-optimal. The areas where time migration constitutes an inadequate imaging solution are those areas affected by significant ray bending; such as directly below steep sided sea-floor canyons, or beneath low velocity geobody lenses. As with any complex or subtle imaging problem, the key to good imaging is the derivation of a representative velocity model. In order to obtain such a model, we must

first produce clean multiple-free pre-stack data. Thereafter, we can resort to pre-stack depth migration (preSDM) to image the subsurface honouring the requisite ray bending.

Here, we demonstrate how velocity model building using a combination of hybrid gridded tomography and detailed manual picking can help resolve the various geophysical challenges encountered in this complex environment, leading to a satisfactory resolution of the imaging problem.

VELOCITY MODEL BUILDING AND PRE-STACK DEPTH MIGRATION

In an environment with small-scale discontinuous velocity anomalies, such as those associated with narrow channel fills or gas hydrate accumulations, a purely layer based velocity model will be inadequate (Jones, 2003, Fruehn et al. 2007). Furthermore, a purely gridded approach may also encounter problems (Jones et al, 2007). A layer based approach assumes that all major velocity changes are bounded by geologic horizons: this can be appropriate for older consolidated sediments, as long as we do not have significant velocity variation with layers (other than a well behaved vertical compaction gradient). A gridded model represents the subsurface velocity distribution with a 'cloud' of values, decoupled from the sedimentary layers. It is of particular value in environments where the velocity field is dominated by the hydrostatic pressure gradient (typically in younger sediments), with velocities increasing more or less monotonically below the sea bed. However, when we encounter significant lateral changes in compaction gradients (as in chalk layers in the North Sea), or have punctual intrusive bodies (such as salt in the Gulf of Mexico or basalt) then both the purely layered and gridded approaches face limitations. The hybrid gridded approach (Jones, et al, 2007) attempts to combine both techniques, by employing a gridded tomographic solver, but inserting layer constraints on the subsequent velocity update.

In this project, we used a hybrid-gridded approach, where we combined conventional gridded tomography, high resolution gridded tomography, autopicked layers to serve as constraints within the tomography, and detailed manually interpreted layers to be inserted as the tops and bottoms of distinct regions were a sufficiently resolved tomographic solution proved unobtainable. In this context, 'high resolution' refers to solving the tomographic problem with 200 m cell dimension in x and y, and 20 m vertically, rather than the more usual 500 m lateral cell dimension with 100 m vertically. The initial depth interval velocity was derived from the preSTM time-stacking velocity (smoothed and converted to depth interval velocity), and the water bottom was autopicked from a water-velocity depth migration and inserted in the initial model as an explicit layer. The water velocity was selected from a migration-perturbation scan (i.e. a suite of migrations using a percentage perturbation about some initial velocity function). As a result of this analysis, a constant value of 1500 m/s was selected. In neighbouring areas, we have noted that a velocity gradient in the water can be of use in imaging the sea bed, but here this was found unnecessary. Following this, several iterations of gridded tomographic model update were performed. This involves running an autopicker (in this instance based on plane-wave destructors: Claerbout, 1992; Hardy, 2003) on densely sampled Kirchhoff preSDM common reflection point (CRP) depth gathers, and inputting the autopicked velocity errors and dip information to the gridded tomographic 3D solver. The solver uses a conjugate gradient (CG) technique to handle large volumes of 3D picks in the tomographic solution. For the model building and the final migration, an amplitude preserving Kirchhoff implementation was used.

In Figure 2, we see a crossline from the 2004 vintage 3D Kirchhoff preSTM showing the complex sea bed structure, and evidence of the structural imprint of shallow sediment velocity anomalies (dimming and pull-down indicated by the circles). The 2004 time migration project used a dense autopicked velocity field as part of the large-scale exploration project undertaken in the region by Reliance Industries. Figure 3 shows an inline from the vintage 3D preSTM. Many near-surface velocity anomalies are evident; some associated with possible gas hydrate accumulations. The shallower (white) ellipse highlights a low velocity geobody, which we infer has a possible component of free gas accumulation associated with the gas hydrate sealing layer as well as possible channel-fill water saturated clay. Beneath this geobody we have a region of dimming and can also note velocity-related pull-down associated with this feature. The deeper ellipse highlights a zone degraded by remnant multiples. Due to the degraded primary signal content resulting from the overburden velocity anomaly, the multiple energy dominates the contribution to the data in the deeper part of the section. Unless we can successfully attenuate the multiple, we would be unable to reveal the underlying geological structure. Aliasing of the multiple moveout behaviour in deep water results in a stack response showing a broken reflector character. For successful model building, such noise must first be removed in the pre-stack domain, and in the preSDM project described here, 3D SRME was successfully employed to achieve this.

In Figure 4, we see the same inline as in Figure 3, after final 3D preSDM imaging with all pre-processing (including 3D SRME). The pull-down has been resolved, and deeper imaging improved (indicated in the ellipse at about 4 km depth). In order to achieve this imaging improvement, the velocity model building required several phases employing different techniques. Firstly, three iterations of purely gridded high resolution CG tomography were employed to refine the sediment velocity field below the autopicked (highly structured) sea bed. These iterations used picks with a 200 m by 200 m lateral and 20 m vertical spacing. Following this, CG tomography (on a 500 m by 500 m by 100 m grid) was used to determine the velocity structure in the larger and deeper low-velocity geobodies (lying mostly a kilometre or more below the sea bed). In some areas, a series of Mio-Pliocene channels were visible, and these were resolved by detailed manual picking in conjunction with a migration velocity-perturbation scan.

Gas hydrates

Clathrates, such as methane hydrates, often form in deep water regions with unconsolidated sediments when the temperature and pressure are appropriate (Carcione and Tinivella, 2000; Chopra et al, 2003). In this area of offshore India, they can occur below a water depth of about 600m (Chaudhuri et al, 2002). The clathrate itself forms an impermeable high velocity (usually thin) layer, and below this, we sometimes see an accumulation of free gas, giving rise to a low velocity zone immediately below the high velocity clathrate layer. A seismic characteristic of these accumulations is that they can cross-cut the sedimentary layering, (so can look like a multiple or remnant bubble-energy in that regard) and they occur about 150 - 250 metres below the sea bed (as indicated in Figure 5). As a reflection event, they sub-parallel the sea bed and are referred to as a ‘bottom simulating reflector’ (BSR). The BSR forms when temperature and pressure conditions are such that clathrates form. These frozen typically methane hydrate structures can cross-cut the geological strata, and given that they are primarily controlled by the hydrostatic pressure gradient below the sea bed, they will tend to be sub-parallel to the sea bed contours. Hence we will see a reflector tracking the sea-bed structure, cross-cutting the sedimentary depositional layers. For velocity anomalies related to the gas hydrate, we relied primarily on high resolution gridded tomography, and were able to

resolve small-scale velocity features (scale length of < 1 km) with interval velocity about 1250 m/s in the underlying free gas zones, compared with the background sediment velocities of about 1600 m/s. These possible free-gas accumulations (or water-saturated clays) have an associated pull-down in the time section as well as amplitude dimming and loss of high frequencies.

Figure 5 details the analysis of a probable gas hydrate accumulation and associated free-gas zone. In the time migration image (left) we can discern an event parallel to the sea bed about 200 m below the sea floor (denoted by the dotted orange line), which is probably a BSR, characteristic of gas hydrate formation. In the corresponding image from the depth migration (center panel), the resolution of the detailed velocity structure helps to clarify the deeper part of the image and to resolve associated pull-down. The vertical white line indicates where we have extracted the velocity profiles associated with the preSTM and preSDM velocity models. These profiles are plotted on the right of the figure. The preSTM profile is smooth and featureless, but the preSDM profile shows a high velocity kick at about 1600 m depth (~250 m below the sea bed), immediately followed by a low velocity zone of about 300 m vertical extent: these features are characteristic of free-gas accumulation below a high-velocity gas hydrate cap, and have been encountered elsewhere in this region. When overpressured, such gas accumulations can constitute a severe geo-hazard.

In Figure 6, we see the initial model (picked sea bed and smooth velocity field from the vintage preSTM) superimposed on the associated 3D preSDM result. The shallow sediment package encircled causes a pull-down in the underlying sediments (highlighted by the deeper ellipse). By the second iteration of tomography, we begin to resolve this pull down as the tomography yields a low velocity geobody, with a minimum interval velocity of ~1300 m/s compared to the surrounding sediment velocity of 1600 m/s (Figure 7).

Channel fills

For intricate narrow channels present in the Mio-Pliocene section just below the sea bed, we relied on manual interpretation of the top and base of the channel features to define their geometry, combined with a scan over potential channel-fill velocities. Due to the small scale of these features, a purely gridded tomographic approach was unable to resolve the required detail. The channels were picked on a dense localized grid of inlines and crosslines. Figure 8 shows the first kilometre of data near the sea bed, where we see deeply incised sea-bed canyons, but also some small localised channels just below the sea bed. These channels result in a severe pull-down distortion of the underlying sediments due to their low-velocity fill. If we were to use a smooth velocity model, we would be unable to resolve these small-scale features (typically 300 m – 400 m in width) hence detailed manual picking is required. The 3D preSDM image shown in Figure 8 was created using a smooth background velocity field (hence the pull-down is visible). The detailed channel-fill velocity model is superimposed (not the velocity used for this migrated image). A migration velocity-scan was used to determine the best channel-fill interval velocity: in this case 1200 m/s was used.
Figures 9 and 10 compare the 3D preSDM results after migrating with a smooth background velocity field (no punctual channels included) versus the result incorporating the low-velocity fill channels. The improvement in the deeper section, below about 2 km depth, is significant. We have not perfectly resolved the shallow channel problems, but incorporating them in this way enables better resolution in the deeper section. Ignoring them is not a viable option.

Underlying low-velocity canyon fills

Below the younger Pleistocene section we have channel-like features, which may be sand-bearing and possibly gas-charged, and could be potential exploration targets, or alternatively could be water-saturated clay bodies (see for example the geobody highlighted in the yellow ellipse in the upper right of Figure 4). These were also the focus of some attention, and high resolution tomography was employed to define some of these features.

In Figure 11 we see CRP gathers and the associated preSDM image with velocity overlay. The velocity here is from a purely gridded CG tomography on a 500 m by 500 m by 100 m input pick cell size. A thin sand lens (50m thickness) can be seen in the lower image, but has not been resolved in the current iteration. The gathers shown in the upper portion of the figure are under-corrected at the top of the lens feature (velocity at this depth too low) and the gathers for the base of the event are flat. Conceptually, we can imagine that increasing the velocity above the feature (so as to flatten the gathers for the top of the channel) will cause the base channel gathers to curl down (too fast), so we also need to reduce the channel fill velocity whilst increasing the velocity above the channel. This has been accomplished in the next iteration (as shown in Figure 12), where the lateral dimensions of the tomographic cell were reduced to 200 m, and the vertical dimension to 20m. We consider this to be close to the vertical resolution of our technique

Model evolution

In the following figures, showing a long crossline adjacent to that of Figure 2, we summarize the evolution of the model: Figures 13 (top and bottom) compare the first and second iterations, which dealt only with the shallow section, whilst Figures 14 and 15 compare the overall section. By the 5th iteration the deep section has been improved considerably. During the model building of the shallow section, the data pre-processing was ongoing, so as to apply lengthy processes such as 3D SRME and the other de-noise steps. These fully pre-processed data were then used for deeper model update and the final imaging. As a consequence, the data input to the earlier model building iterations did not have the full de-noise pre-processing sequence applied. This is reasonable for deep water environments, as we have a lot of work to do in model building before encountering the first multiple. Overlapping the pre-processing and model building in this way also facilitates reduction of overall turnaround time.

It is important to note that for a global tomographic solution, all parts of the model can be adjusted at each iteration. Hence we can see subtle changes in the shallow section for some parts of the model even at the latter iterations. Once we have imposed a layer constraint in the hybrid scheme (such as for the sea bed, or detailed picked channels), then those parts of the model remain invariant, and the update scheme ceases to be a truly global one and thus can be viewed as a class of layer stripping (although we have much more flexibility in a gridded scheme than in a purely layer based scheme).

CONCLUSIONS

For imaging in complex environments, it is necessary to employ a wide range of tools for suppression of the various classes of noise and multiples. This must be accomplished in the pre-stack domain so that automated dense picking can be performed on migrated gathers to permit reliable model update. In deep water areas, we are fortunate that the water bottom multiple problem does not affect much of the data, so we can proceed with model building for the data above the time of the first water bottom multiple, whilst demultiple processing is

proceeding in parallel. However, we still need to address internal multiple and other noise problems. In addition, a flexible approach to model update is required, permitting us to incorporate small-scale punctual velocity features such as those associated with low-velocity channel fills, as well as resolving the gradational lateral and vertical changes associated with broader structural trends. At some short scale lengths, a tomographic solution is unlikely to be able to resolve important velocity detail, and in these instances it is important to be able to incorporate velocity information from other sources. In this case study, we have embedded into the model, a network of narrow channels, defined by detailed picking of their tops and bases from a dense grid of inlines and crosslines.

Utilization of such an approach for data offshore eastern India has resulted in an improvement in image quality compared to a recent pre-stack time migration, avoiding the structural distortion introduced by localized velocity variation in the near surface sediments.

ACKNOWLEDGEMENTS

Our thanks to colleagues at Reliance Industries and ION GX Technology for help and advice during this project, especially to Phil Smith at GXT who ran the pre-processing, and to our respective employers for permission to present this work. Thanks also to the SEG reviewers, Andreas Rüger, Sylvestre Charles, and Editor Tamas Nemeth and Associate Editor Bill Harlan for their insightful comments and encouragement with this publication.

REFERENCES

Carcione, J. M., and U. Tinivella, 2000, Bottom-simulating reflectors: Seismic velocities and AVO effects: Geophysics, **65**, 54-67.

Chaudhuri, D., N. Lohani, S. Chandra, and A. Sathe, 2002, AVO attributes of a bottom simulating reflector: East coast of India: 72nd Annual International Meeting, SEG, Expanded Abstracts, 300-303.

Chopra, S., V. Alexeev, and Y. Xu, 2003, Successful AVO and Cross-plotting: Recorder, **28**, no. 9, 5-11.

Claerbout, J. F., 1992, Earth Soundings Analysis: PVI, Blackwell Scientific Publications.

Hardy, P. B., 2003, High resolution tomographic MVA with automation: SEG/EAGE summer research workshop, Trieste.

Fruehn, J., H. Sherazi-Selby, P. Hardy, J. Tryti, and N. Steinsland, 2007, High-resolution velocity model-building for pre-stack depth migration in the Nordsjøn area, Norwegian North Sea: 69th EAGE Conference and Exhibition.

Jones, I. F., 2003, A review of 3D preSDM velocity model building techniques: First Break, **21**, No. 3, 45-58.

Jones, I. F., M.J. Sugrue, P. B. Hardy, 2007, Hybrid Gridded Tomography: First Break, **25**, No. 4, 15-21.

Sangvai, P., A. Biswal, M. Mathur, J. K. Fruehn, P. Smith, D. G. King, I. F. Jones, and M. C. Goodwin, 2008: Complex Imaging Challenges: Offshore South East India: Proceedings of the 7th biennial meeting of the SPG, Hyderabad.

Smith P., I. F. Jones, D.G. King, P. Sangvai, A. Biswal, and M. Mathur, 2008, Deep Water Pre-Processing, East Coast India: First Break, in press.

Stewart, P., 2004, Multiple attenuation techniques suitable for varying water depths: Proceedings of the CSEG annual meeting.

Stewart, P. G., I. F. Jones, P. B. Hardy, 2007, Solutions for deep water imaging: Geohorizons, January, v12, No. 1, 8-22.

Verschuur, D. J., A. J., Berkhout, C. P. A, Wapenaar, 1992: Adaptive Surface Related Multiple Elimination: Geophysics, 57, 1166-1177.

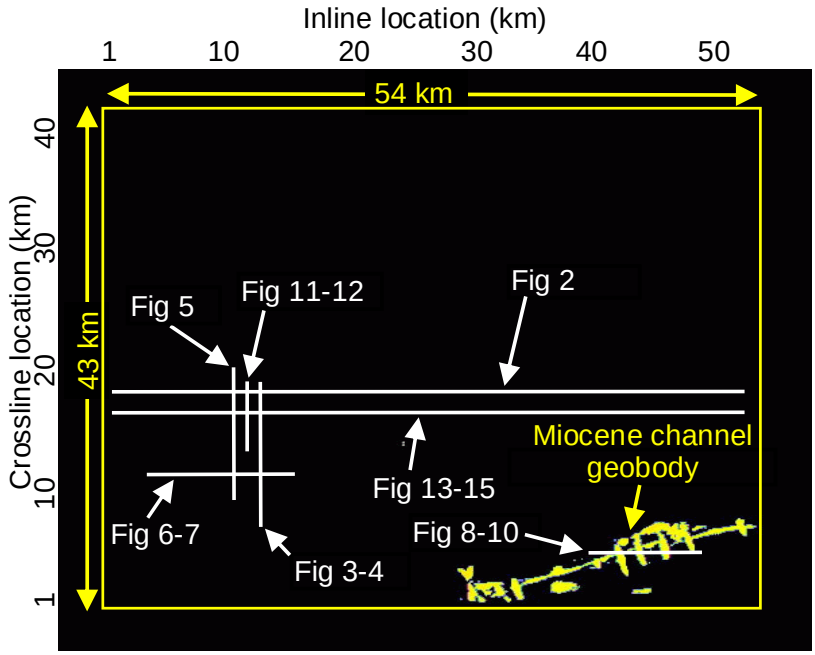

FIGURE 1. Survey map showing various inlines and crosslines described in this paper. Also seen in the lower left is the low-velocity geobody delineated by detailed picking on a grid on inlines and crosslines, outlining shallow canyon-fill sediments.

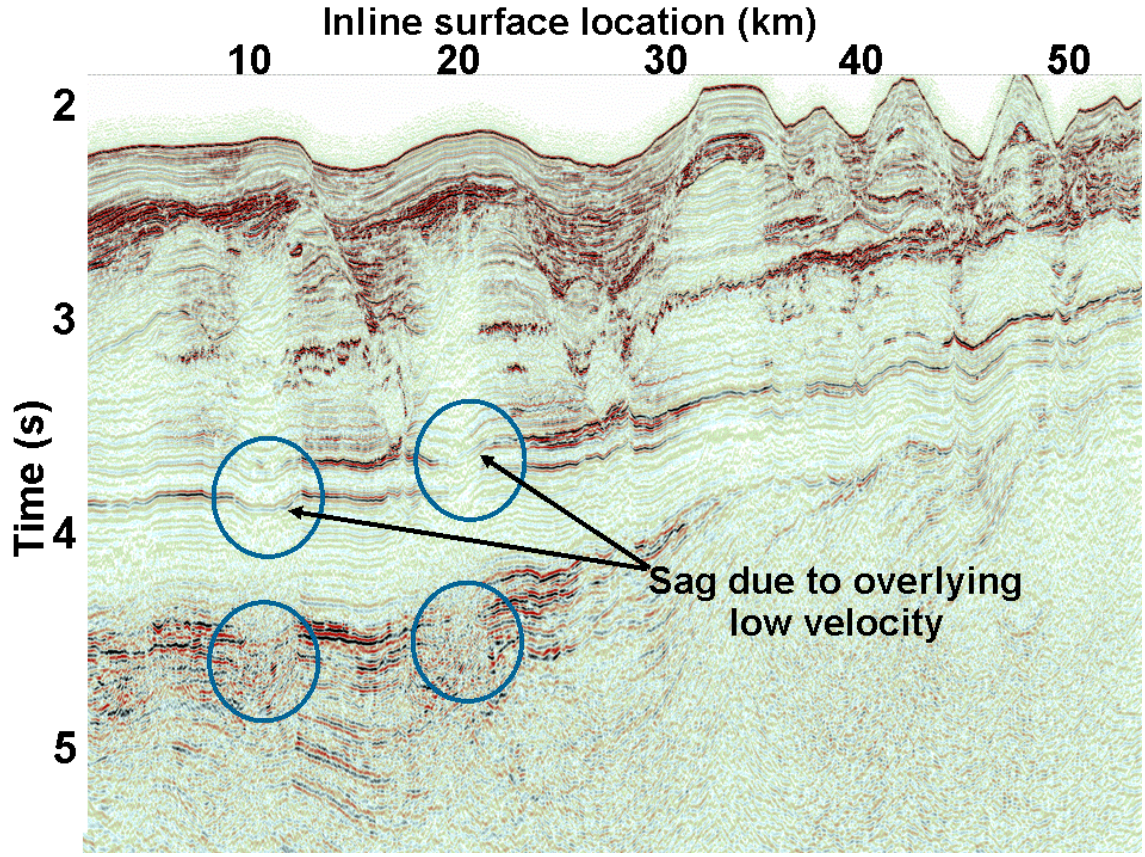

FIGURE 2. 3D crossline from the 2004 vintage 3D Kirchhoff preSTM (with 2D demultiple only), showing dimming and structural pull-down (sag) associated with shallower low velocity anomalies (circled in the shallower part) and associated remnant multiple degradation of the deeper image below (also circled).

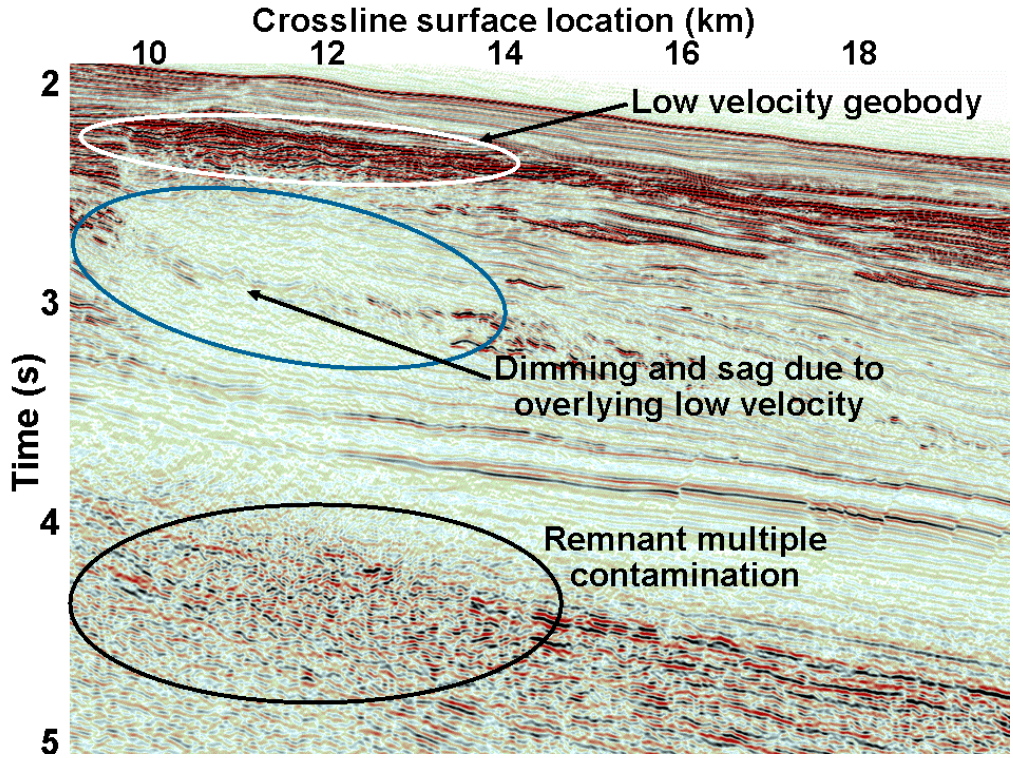

FIGURE 3. Vintage 2004 3D preSTM inline (with 2D demultiple only). Dimming below a shallow geobody is evident (circled), and below, remnant multiple contamination degrades the image (circled).

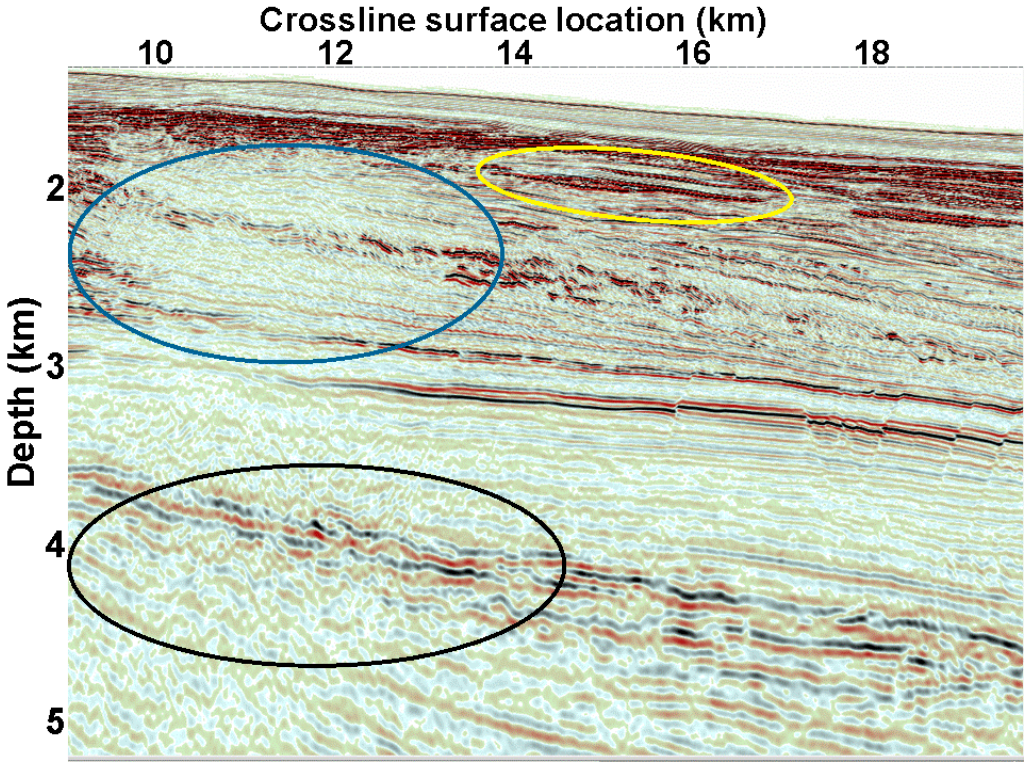

FIGURE 4. New 3D preSDM from same inline as Figure 3, following 3D SRME. The slight sag is mostly resolved, and remnant multiple contamination mostly removed by the 3D demultiple, allowing a reasonable image to obtained. The feature encircled in the rightmost shallow yellow ellipse is described in mode detail in Figure s 11 and 12.

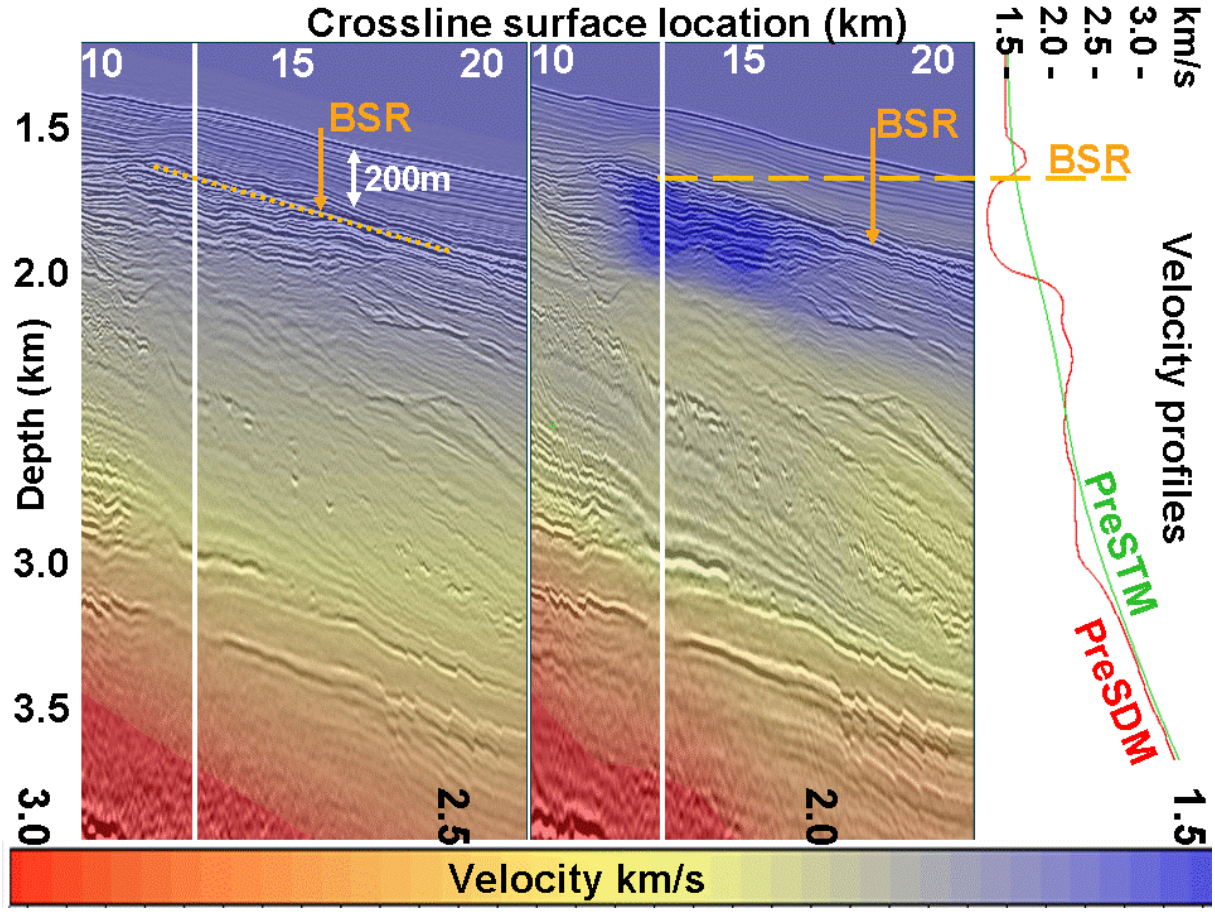

FIGURE 5. The smooth velocity field derived for time domain migration (leftmost preSTM seismic section) does not require high resolution detail. For depth imaging, the velocity estimation techniques used are capable of providing the higher resolution detail required for more demanding depth imaging (central preSDM seismic section). On the right, we see the smooth velocity profile from the preSTM (in green) and also the more detailed velocity profile from the tomographic preSDM model building (in red). This could be interpreted as a characteristic high velocity clathrate cap and underlying low-velocity free gas zone (these observations and inferences are speculative). The locations where these velocity profiles are extracted are indicated by the solid white vertical lines on the seismic sections.

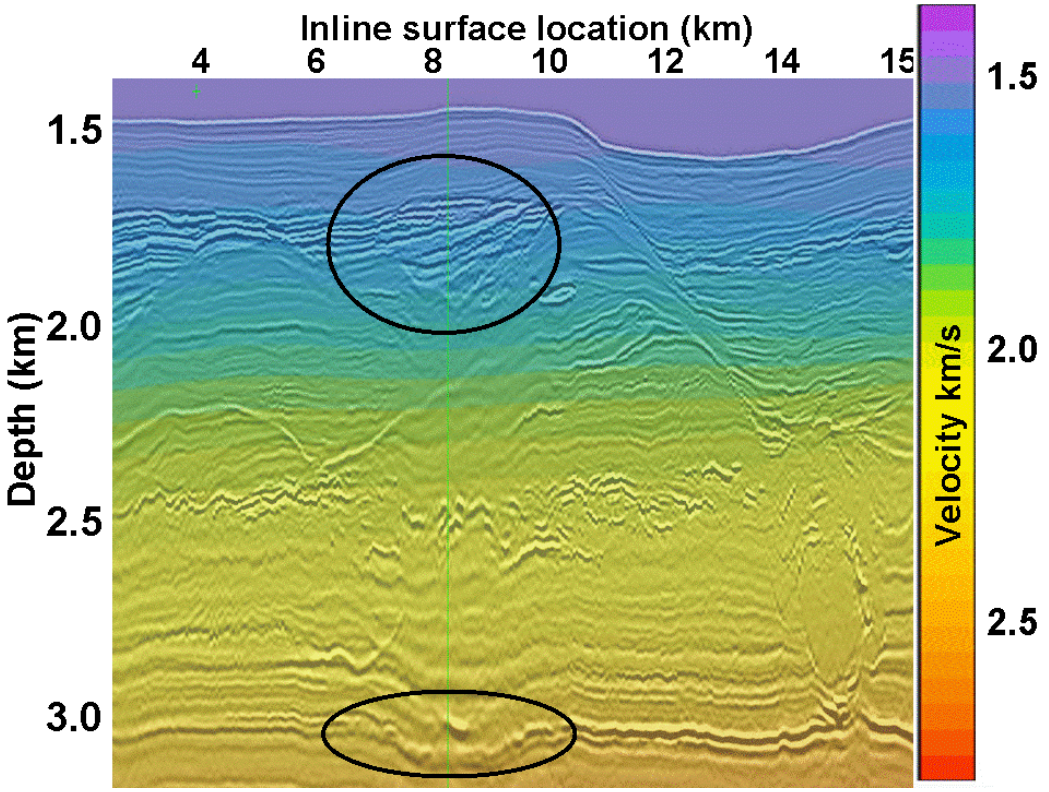

FIGURE 6. 3D preSDM using initial model, showing evidence of pull-down (highlighted in the lower ellipse) resulting from a shallow velocity anomaly (highlighted in the shallower ellipse).

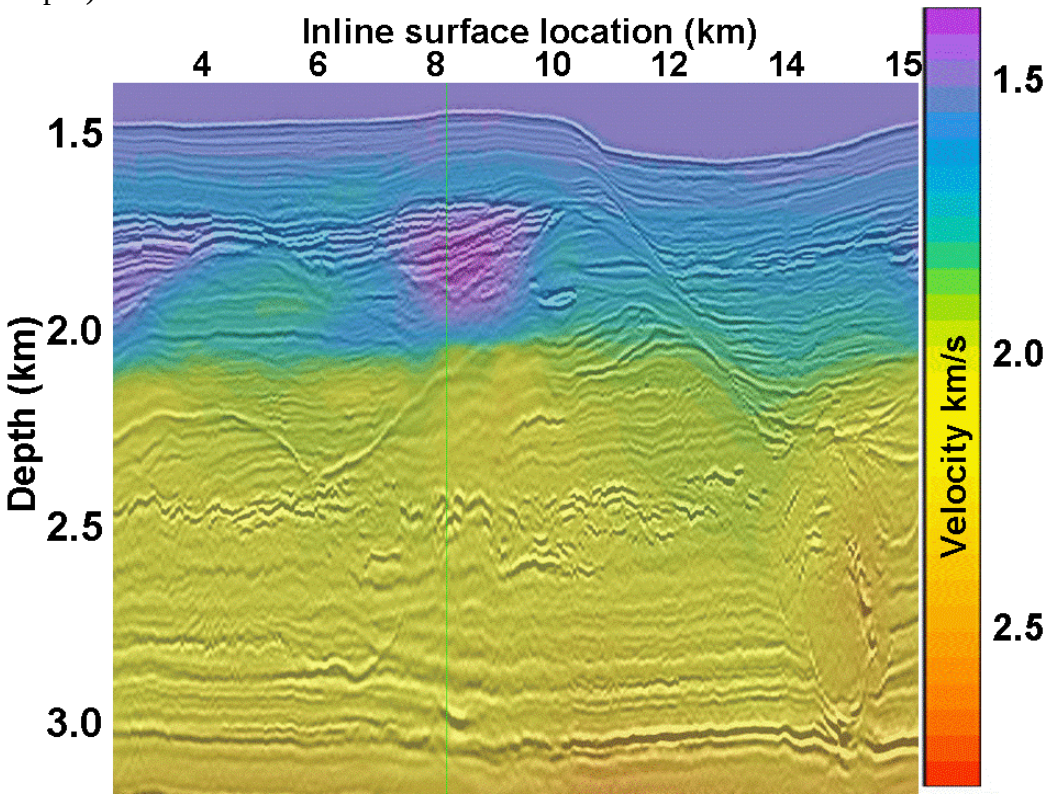

FIGURE 7. 3D preSDM after second iteration attempting to resolve pull-down. The pull down near 3 km depth has been mostly corrected, as the velocity in the shallow geobody has been reduced from about 1600 m/s to ~ 1400 m/s.

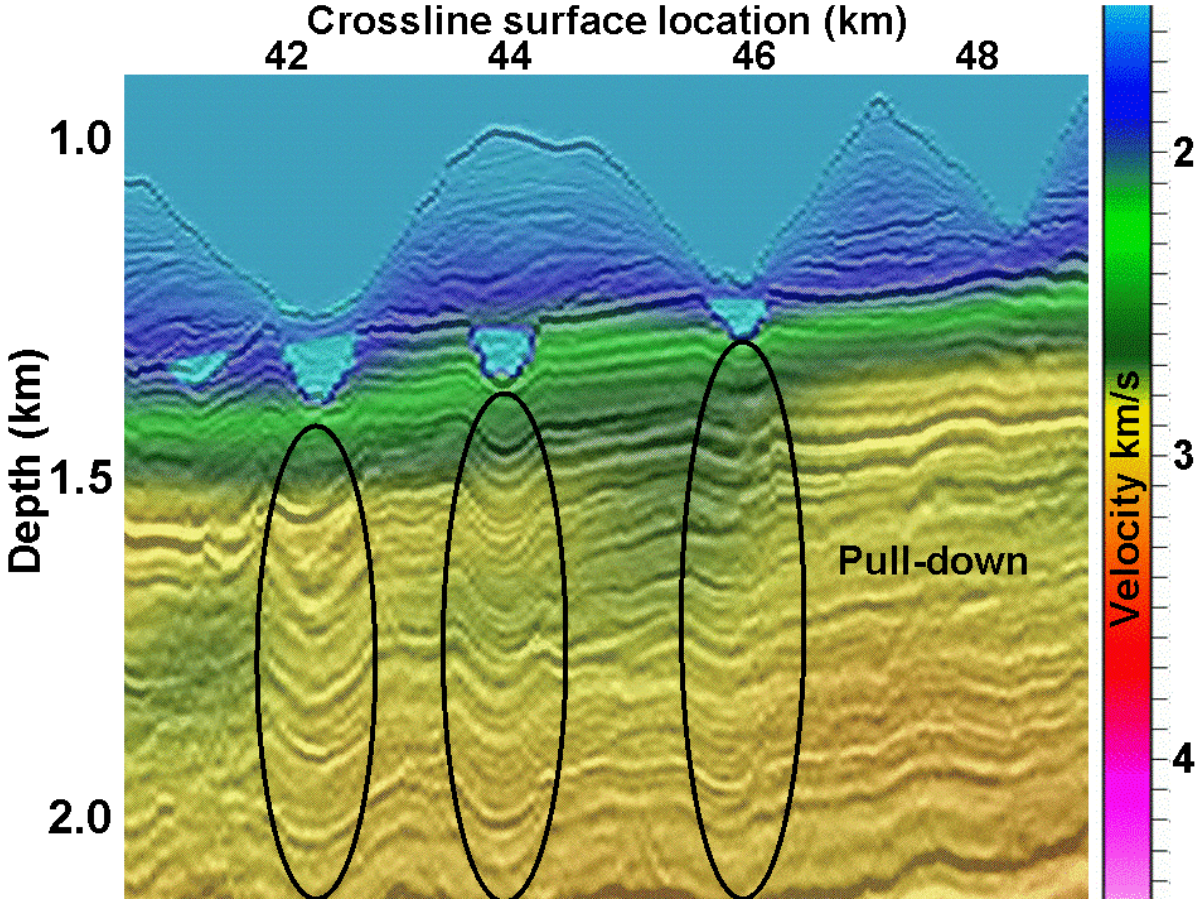

FIGURE 8. Picked canyon-fill events (four pale blue features just below the sea bed) with color overlay of the final selected velocity-fill model, superimposed on an initial preSDM crossline produced using a smooth velocity model (hence clearly showing the pull-down problems).

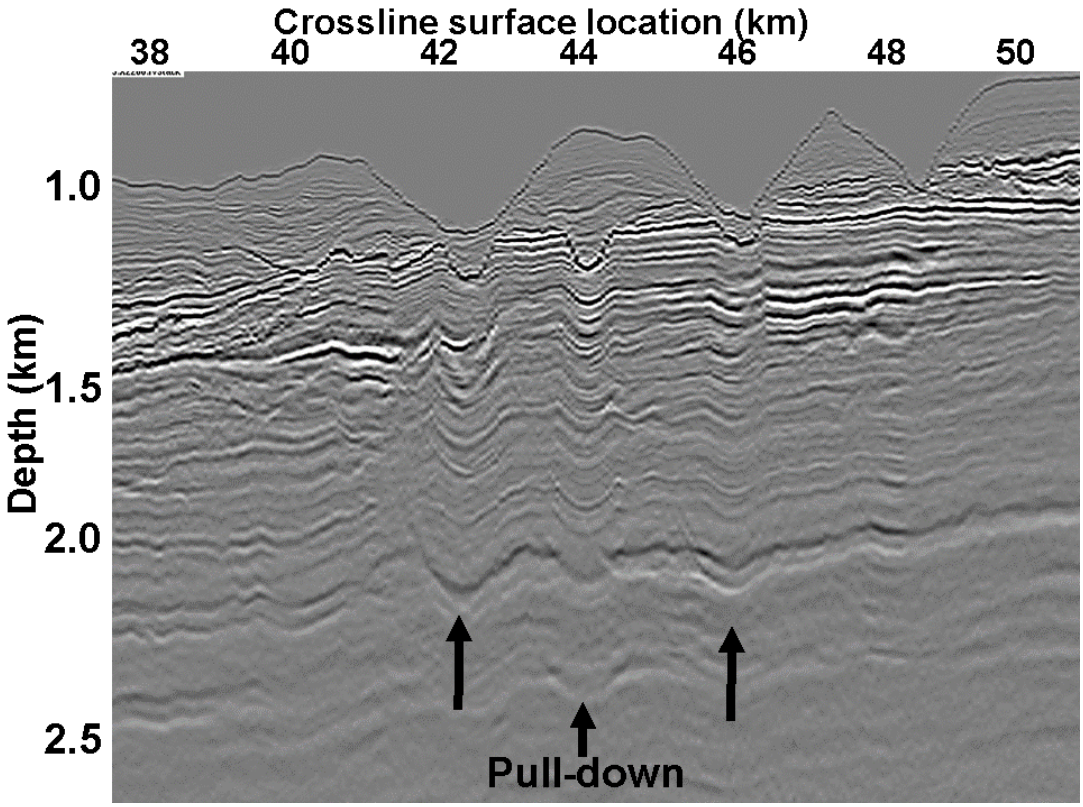

FIGURE 9. 3D preSDM crossline with smooth background model: numerous probable pull down features can be identified. Imaging below these features is problematic.

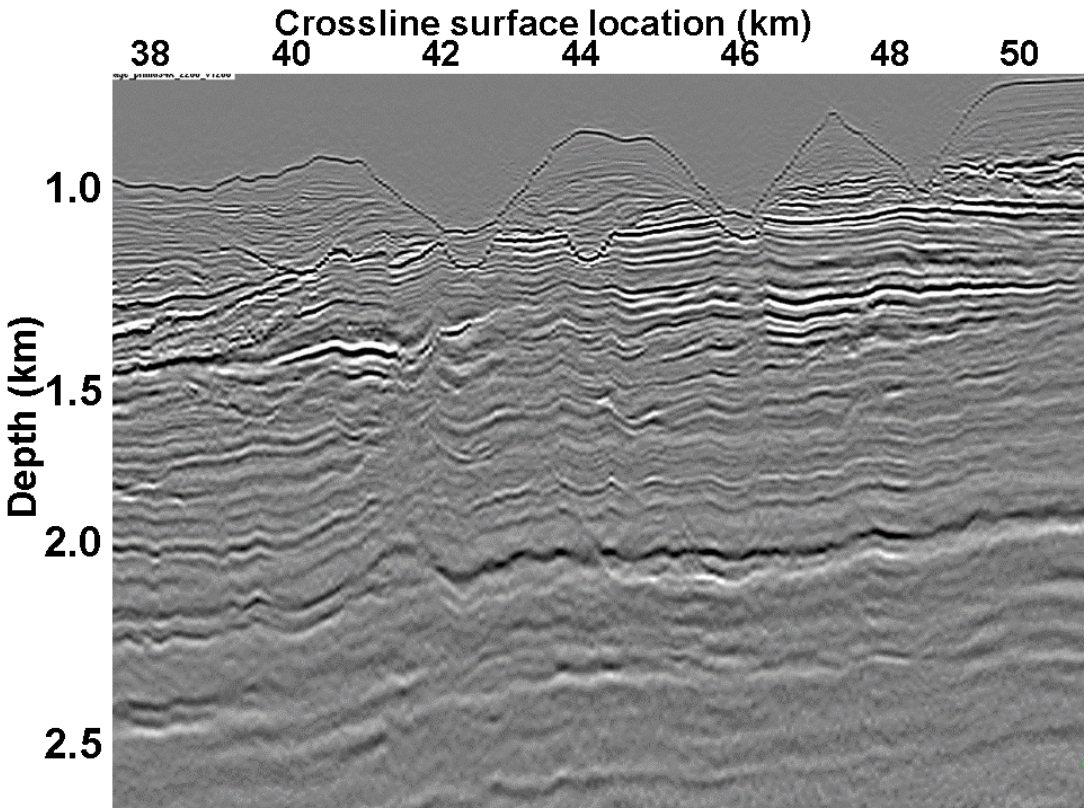

FIGURE 10. 3D preSDM crossline with detailed low-velocity channel-fill model: sags greatly reduced, and deeper imaging is clearly improved.

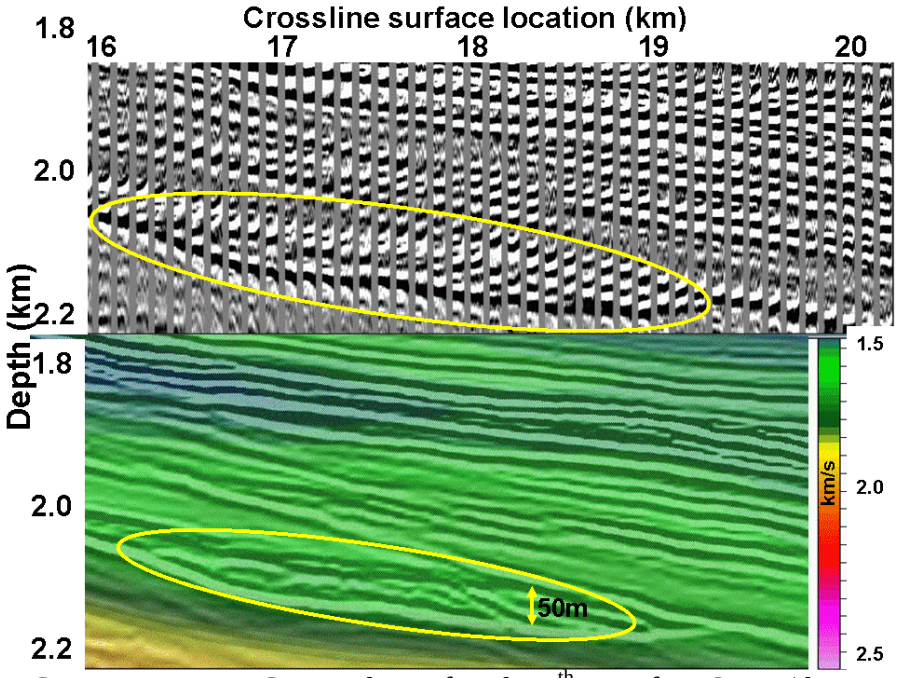

FIGURE 11: Top: CRP gathers after the 4th run of preSDM (these gathers are used as input to the next iteration of tomographic model update). We can see some residual velocity error (gathers curling upwards = velocity still too low) above the channel. Bottom: image associated with these gathers with interval velocity color overlay. The thin lens feature (encircled) is seen in a larger context in the upper right of Figure 4.

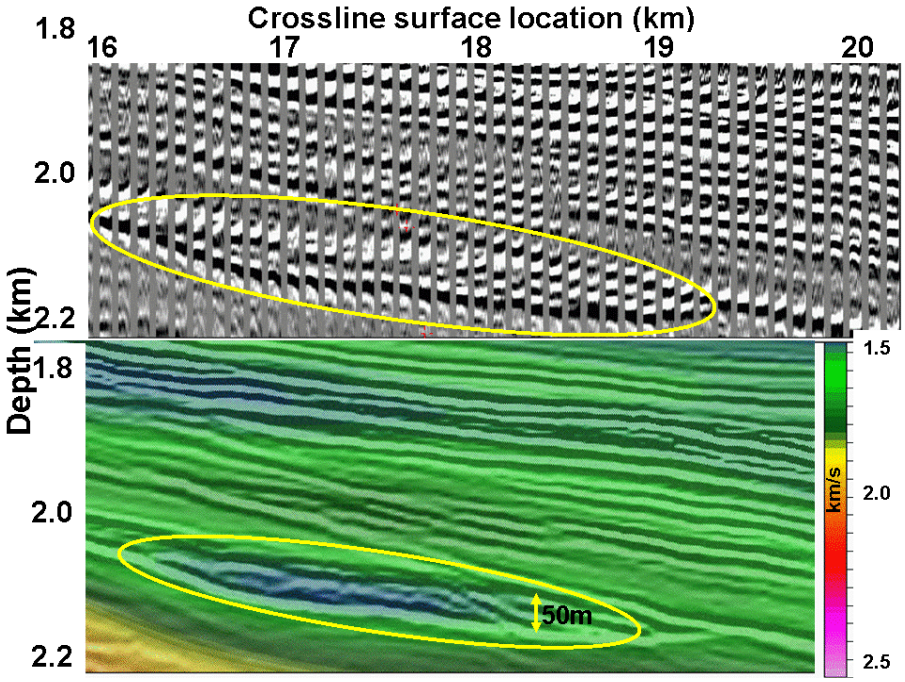

FIGURE 12. Top: CRP gathers after the subsequent update of 3D CG tomography. Some of the under-correction above the channel has been resolved, and the channel velocity itself lowered, so as to preserve flat gathers at the channel base. Bottom: image associated with these gathers with interval velocity color overlay, showing the low velocity in the thin channel feature. The thin feature (encircled) is seen in a larger context in the upper right of Figure 4.

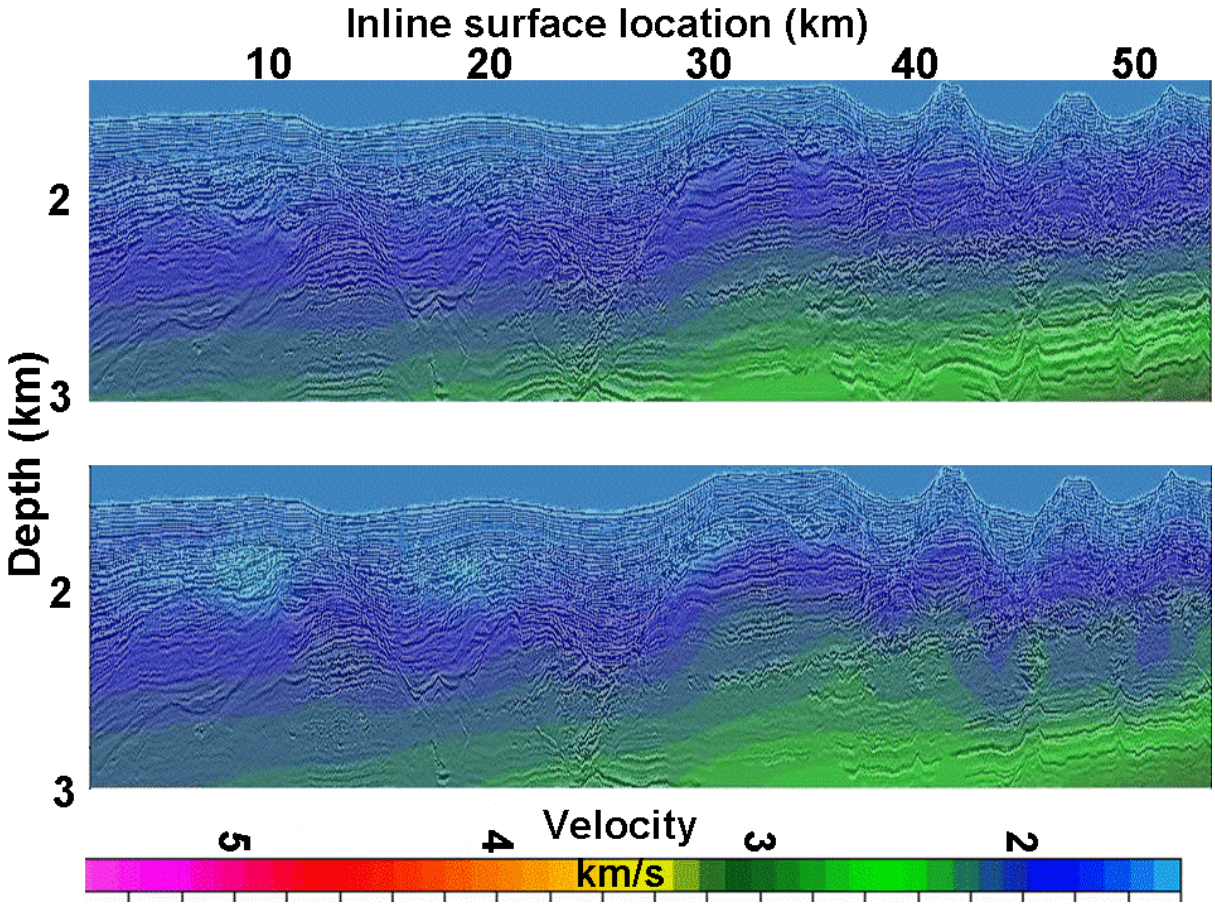

FIGURE 13. Upper panel: first iteration of model update for preSDM crossline down to 3 km. Lower panel: second iteration of model update down to 3 km. For the most part, the structural imprint of the sea bed and underlying sediments has been removed. Both images shown with interval velocity color overlay.

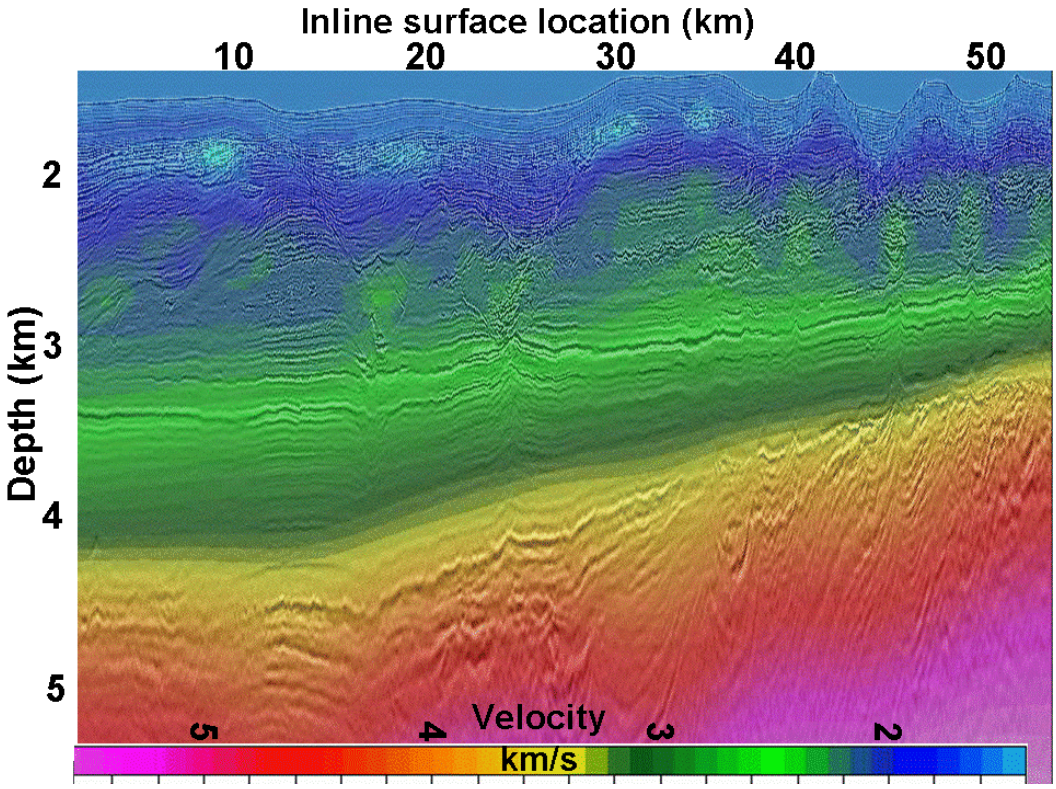

FIGURE 14. The whole crossline section for iteration 4, with interval velocity color overlay.

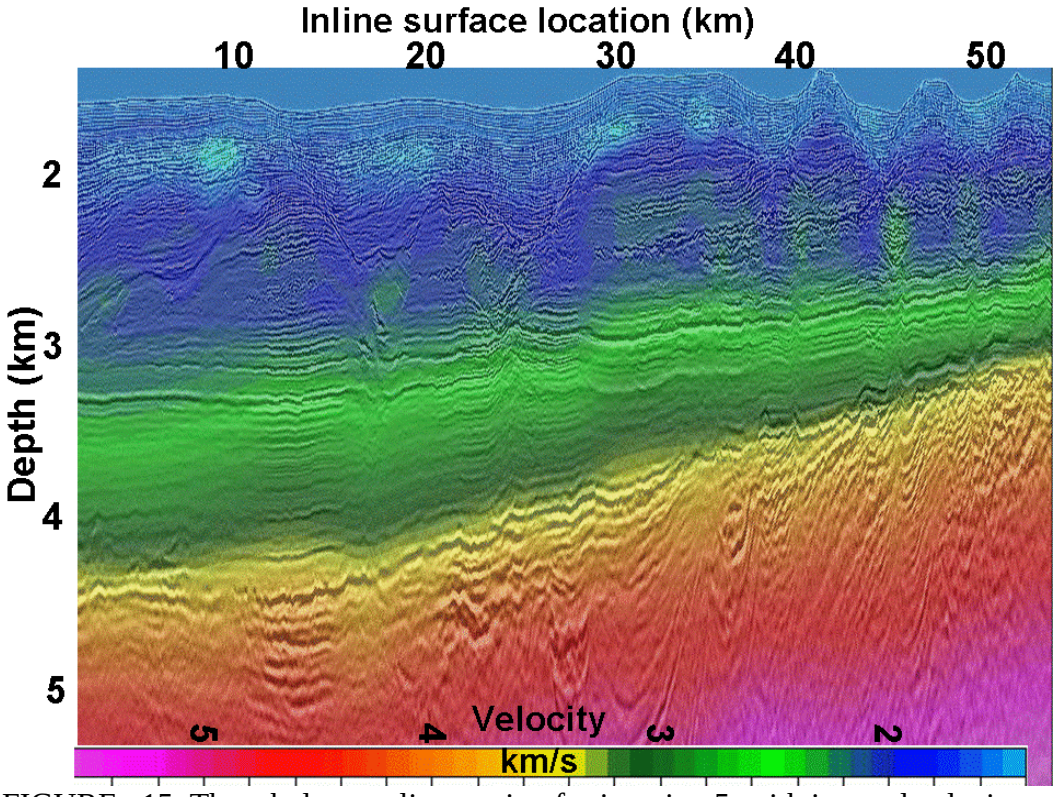

FIGURE 15. The whole crossline section for iteration 5, with interval velocity color overlay. The majority of the structural imprint of the overburden has been removed.